International Journal of Control

ISSN: 0020-7179 (Print) 1366-5820 (Online) Journal homepage: https://www.tandfonline.com/loi/tcon20

Tracking the gradient of artificial potential fields: sliding mode control for mobile robots

JÜRGEN GULDNER & VADIM I. UTKIN

To cite this article: JÜRGEN GULDNER & VADIM I. UTKIN (1996) Tracking the gradient of artificial potential fields: sliding mode control for mobile robots, International Journal of Control, 63:3, 417-432, DOI: 10.1080/00207179608921850

To link to this article: https://doi.org/10.1080/00207179608921850

INT. J. CONTROL, 1996, VOL. 63, NO. 3, 417–432

Tracking the gradient of artificial potential fields: sliding mode control for mobile robots

JÜRGEN GULDNER† and VADIM I. UTKIN‡

Artificial potential fields and artificial force fields are widely used in robotics for path planning and collision avoidance, both for robot manipulators and for mobile robots. Despite intensive research in designing suitable artificial potential fields, little attention has been devoted to tracking control for following the gradient of an artificial potential field. However, good tracking control is vital for successful application of the artificial potential field method in order to guarantee safe operation of the robot. In this paper, we extend previous results on a sliding mode control strategy to include actuator dynamics and non-holonomic motion constraints of mobile robots into the gradient tracking control algorithm.

1. Introduction

Artificial potential fields and artificial force fields are a widespread tool for path planning and collision avoidance of robotic systems. The main idea is to construct an artificial potential function with a gradient field attracting the robot to the target position or the goal point while also repelling the robot from obstacles in the workspace. Artificial potential fields were made popular by Khatib (1986) and were subsequently utilized in a number of studies both for robot manipulators and for mobile robots. Provided the artificial potential function is designed adequately, motion along its gradient is guaranteed to be free of collisions with obstacles in the workspace. Among the many approaches motivated by Khatib's fundamental research are elliptical potentials, introduced by Volpe and Khosla (1987); superquadratic potentials, presented by Khosla and Volpe (1988), and navigation functions, see Koditschek (1987) and Rimon and Koditschek (1992).

Despite the vast number of artificial potential fields proposed in the literature, few works discuss suitable control for tracking the gradient of an artificial potential field or, more generally, for tracking a smooth artificial vector field. This deficit is surprising since good tracking control is vital for successful implementation of the artificial potential field method. On the other hand, numerous tracking controllers have been proposed for n-link robot manipulators. An explicit equation of the desired trajectory generally serves as the reference input; hence, these control algorithms are not suitable for gradient tracking.

In most of the previous research on artificial potentials, the gradient was directly coupled into the system dynamics, 'implementing a dynamic relationship between the robot and its environment', as described by Hogan (1985). Effectively, the control

Received 8 August 1994. Revised 19 December 1994.

† Institute for Robotics and System Dynamics, DLR, German Aerospace Research Center, Postfach 1116, D-82230 Wessling, Germany.

‡ Department of Electrical Engineering, Ohio State University, 2015 Neil Avenue, Columbus, OH 43210-1275, U.S.A.

forces/torques act colinear to the gradient, which obviously does not result in tracking of the gradient lines. The term 'gradient lines' denotes the trajectories obtained by exactly following the gradient of an artificial potential field. However, the explicit equations of the gradient lines do not have to be derived for obstacle avoidance using the artificial potential field method. For potentials tending to infinity at obstacle boundaries, no collisions will occur even in the face of actuator limitations, as shown by Rimon and Koditschek (1992). In an effort to achieve tracking of the gradient lines, feedback linearization was proposed by Khatib (1986) under the assumption of exact knowledge of the system dynamics. Koditschek (1991 a, b) eliminated the requirement of exact knowledge using the natural motion approach for fully actuated robots. Still, external forces like gravity have to be known exactly and the gradient of the navigation function employed by Rimon and Koditschek (1992) depends implicitly on the robot inertia matrix.

In many applications, it is desirable to be able to directly design the artificial gradient independently of the robot inertia matrix, requiring efficient tracking control. In Utkin *et al.* (1991) and Hahimoto *et al.* (1993), a sliding mode controller was introduced for fully actuated robotic systems. The sliding mode controller was applied to gradient tracking control of holonomic robots by Guldner and Utkin (1993, 1995), under the assumption that the input forces/torques can be varied discontinuously. This is not feasible in real-life mechanical systems, where unmodelled dynamics, for example those of actuators, impose limits on the bandwidth of the controller. In particular, unmodelled dynamics are known to cause chattering in systems with sliding mode control, which is extremely harmful to mechanical system components.

The present study discuss extensions of the theoretical results of Guldner and Utkin (1993, 1995) (see §2 for a brief summary) to practical applications. The control objective considered in this paper is to track the planar gradient of an artificial potential field with real-life mobile robots. Suppression of chattering triggering by actuator dynamics is achieved by introducing asymptotic state-observers as a bypass for the high frequency component in the sliding mode control signal, as shown in §3.

Furthermore, most prototypes of mobile robots have non-holonomic kinematics, which require additional considerations for designing the control algorithm. A non-holonomic wheel-set is used to illustrate the control design for this case in §4.

2. Tracking the gradient of an artificial potential field

In this section, we recapitulate the sliding mode controller for gradient tracking, originally presented by Utkin *et al.* (1991). The controller version described below is based on an abstract point-mass model for a mobile robot, neglecting actuator dynamics. The goal of this section is to enhance the understanding of the methodology of control design for real-life mobile robots with actuators and non-holonomic kinematics presented in the later sections of the paper.

2.1. *Potential field requirements*

In general, the control methodology presented here can be applied to the tracking of any artificial vector field, provided some smoothness conditions are fulfilled. In an effort to avoid tedious derivations of such smoothness conditions, we restrict the development to gradients of potential functions. We assume that the gradient lines are

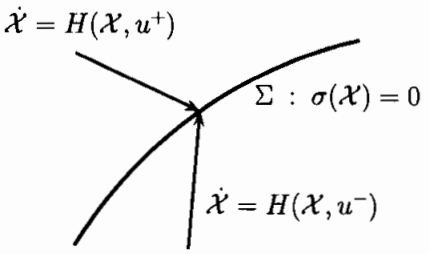

Figure 1. State vectors in the vicinity of the sliding manifold.

sufficiently smooth to enable tracking under the given kinematic constraints and control resource limitations. In other words, the curvature ρ of the gradient $\mathscr{E} = -\nabla\mathscr{U}$ of the potential field $\mathscr{U}$ is assumed to be upper bounded by a known scalar $\rho^+ > 0$.

2.2. *Abstract point mass model*

In the initial works (Utkin *et al.* 1991, Hashimoto *et al.* 1993), a sliding mode controller was designed for fully actuated, holonomic robots with n degrees of freedom. For mobile robots operating in the plane, the sliding mode gradient tracking control algorithm assumes an abstract point mass model without an orientational degree of freedom. The motion of a potent mass M is described by

$$M\begin{bmatrix}\ddot{x}\\ \ddot{y}\end{bmatrix} + g(x, \dot{x}, y, \dot{y}) = f \tag{1}$$

where $(x, y) \in \mathbb{R}^2$ describes the location of the mobile robot with respect to a fixed reference coordinate system, $g(x, \dot{x}, y, \dot{y}) = [g_x(x, \dot{x}, y, \dot{y})\ \ g_y(x, \dot{x}, y, \dot{y})]^T$ comprises all additional dynamic effects such as centripetal, Corriolis and friction, and $f = [f_x\ f_y]^T$ are mechanical control forces.

We assume that the euclidean norm (denoted by $\|\cdot\|$ throughout the paper) of the vector $g(x, \dot{x}, y, \dot{y})$ is bounded for all operating conditions by a known scalar constant

$$\|g(x, \dot{x}, y, \dot{y})\| \leqslant g^+ \tag{2}$$

and that there exist known bounds $0 < M^- \leqslant M \leqslant M^+$ on the robot mass.

The control design of Utkin *et al.* (1991), Hashimoto *et al.* (1993) and Guldner and Utkin (1993, 1995) also assumed negligible actuator dynamics of (1). In particular, the control forces f were varied discontinuously.

2.3. *Briefing on sliding mode control*

Sliding mode control and variable structure control are widely used in linear and nonlinear systems, in particular in robotics. The basic idea is to force a dynamic system

$$\dot{\chi} = H(\chi, u), \quad X \in \mathbb{R}^n, \quad u \in \mathbb{R}^m, \quad m < n \tag{3}$$

to restrict its motion to a sub-manifold of the state-space, called the 'sliding manifold'

$$\Sigma : \sigma(\chi) = 0, \quad \Sigma \subset \mathbb{R}^{n-m} \tag{4}$$

This is achieved by directing the system trajectories towards this manifold 'from both sides' using two different controls u^+ and u^-, as shown in Fig. 1.

The main benefits of sliding mode control are its invariance properties and the ability to decouple high dimensional problems into two sub-tasks of lower dimension: the design of a suitable sliding manifold $\sigma(\chi) = 0$ and of a controller $u \in \mathbb{R}^m$ to enforce sliding mode along the manifold $\Sigma \subset \mathbb{R}^{n-m}$. The interested reader is referred to DeCarlo *et al.* (1988) for a tutorial introduction and to Utkin (1992) for a more detailed discussion on sliding mode theory.

2.4. *The basic gradient tracking controller*

Most previous implementations of artificial potential fields apply forces along the gradient, which amounts to 'specifying a reasonable system behaviour without explicitly specifying system trajectories' (Hogan 1985). The sliding mode controller provides exact tracking of the gradient $\mathscr{E}(x, y) = -\nabla\mathscr{U}$ of an artificial potential field $\mathscr{U}(x, y)$, and is robust with respect to uncertainties and disturbances in the motion equation (1). The key idea is to regard the system velocity vector $[\dot{x}\ \dot{y}]^T$ rather than the system acceleration vector $[\ddot{x}\ \ddot{y}]^T$ as the variable under control. The two-dimensional sliding manifold is defined in four-dimensional state space $[x\ \dot{x}\ y\ \dot{y}]^T$ as

$$s(x, \dot{x}, y, \dot{y}) = \begin{bmatrix} \dot{x} \\ \dot{y} \end{bmatrix} - v_d(t) \frac{\mathscr{E}(x, y)}{\max(\|\mathscr{E}(x, y)\|, \varepsilon_{\mathscr{U}})} = 0 \tag{5}$$

where $v_d(t)$ is a scalar 'travelling' velocity. For $\varepsilon_{\mathscr{U}} < \|\mathscr{E}(x, y)\|$, the right-hand term in (5) reduces to a unit vector colinear to the gradient

$$\frac{\mathscr{E}(x, y)}{\|\mathscr{E}(x, y)\|} \tag{6}$$

In points with $\mathscr{E}(x, y) = 0$, the term (6) would introduce discontinuities into the sliding manifold (5). The sliding mode along $s(x, \dot{x}, y, \dot{y}) = 0$ cannot be provided in discontinuity points with finite control resources since the velocity vector $[\dot{x}\ \dot{y}]^T$ in the robot model (1) is continuous. The small scalar constant $\varepsilon_{\mathscr{U}}$ is employed to smooth the desired direction of motion in the vicinity of singular points $\mathscr{E}(x, y) = 0$ of the gradient.

The goal of control is to track the planar gradient $\mathscr{E}(x, y)$. Restriction of the system to the manifold (5) implies that the velocity vector $[\dot{x}\ \dot{y}]^T$ is oriented colinear to the gradient $\mathscr{E}(x, y)$ with its magnitude being determined by $v_d(t)$, and possibly by $\varepsilon_{\mathscr{U}}$. Consequently, in contrast to approaches with the control force f being colinear to the gradient, the bounded control (7) leads to ideal tracking of the desired trajectories described by the gradient of the artificial potential function.

Control to enforce the sliding mode in the manifold (5) is designed component-wise rather than vector-wise, as in the unit control approach by Guldner and Utkin (1993, 1995). The control forces are assumed to take two symmetric values $f_x \in \{-f_0, f_0\}$ and $f_y \in \{-f_0, f_0\}$. The sliding mode controller is defined as

$$\begin{bmatrix} f_x \\ f_y \end{bmatrix} = -f_0 \begin{bmatrix} \operatorname{sign} s_x \\ \operatorname{sign} s_y \end{bmatrix} \tag{7}$$

The existence of the sliding mode in each of the manifolds $s_x = 0$, $s_y = 0$, and in their intersection, can be established using the Lyapunov function candidate

$$V = \tfrac{1}{2} s^T s = \tfrac{1}{2}(s_x^2 + s_y^2) \tag{8}$$

Differentiating V in (8) with respect to time along the trajectories of the system (1) under control (7), an upper bound on $\dot{V} = s_x \dot{s}_x + s_y \dot{s}_y$ can be found with the help of the bounds in §2.2 as

$$\dot{V} \leqslant \left(\frac{g^+}{M^-} - \dot{v}_d - v_d^2 \rho - \frac{f_0}{M^+} \right) (|s_x| + |s_y|) \tag{9}$$

where the curvature of the gradient

$$\rho = \left\| \nabla^T \cdot \frac{\mathscr{E}}{\max(\|\mathscr{E}(x, y)\|, \varepsilon_{\mathscr{E}})} \right\| \tag{10}$$

is known and was assumed to be upper bounded by $\rho \leqslant \rho^+$ in §2.1. Stability of $s(x, \dot{x}, y, \dot{y}) = 0$ in (5) for given control resources f_0 can be guaranteed by defining the travelling velocity $v_d(t)$ according to

$$\dot{v}_d(t) = a_d^+ - v_d^2(t) \rho \tag{11}$$

with the maximal acceleration a_d^+ being constrained by

$$a_d^+ \leqslant \frac{f_0}{M^+} - \frac{g^+}{M^-} \tag{12}$$

The assumption on the boundedness of the curvature of the gradient, ρ, and the availability of sufficient control resources to enable tracking (see §2.1) ensures that there exists a solution to (11) under constraint (12).

It should be noted that (11) also incorporates proper acceleration in the starting phase for initial conditions $v_d(0) = 0$. Instantaneous generation of sliding mode is achieved for zero initial conditions $s(0) = 0$. In order to achieve proper deceleration at the goal point, the travelling velocity v_d should be chosen as

$$v_d(t) = (2 a_d^+ d(t))^{1/2} \tag{13}$$

in the vicinity of the goal point. $d(t)$ denotes the remaining distance to the goal point. Equation (13) prevents overshoot at the goal point and guarantees a finite approaching time, as proved by Utkin *et al.* (1991) and Hashimoto *et al.* (1993). In addition, v_d should be bound by $|v_d| \leqslant v_d^+$ according to the specifications of the mobile robot used.

2.5. *Implementational issues*

Two obstacles hinder direct implementation of the above control algorithm in real-life mobile robots.

(*a*) The control law (7) assumes discontinuous control forces f that cannot be implemented with finite actuator resources. The actuator dynamics will be excited by the discontinuous control, resulting in chattering.

(*b*) Model (1) is only valid for fully actuated, omni-directional mobile robots since the orientational degree of freedom is neglected. A number of prototypes of mobile robots, however, have tricycle kinematics and are subjected to non-holonomic motion constraints. Therefore, the point mass model (1) is not appropriate.

In the following two sections, we will discuss the effects of these peculiarities on the gradient tracking control design procedure.

3. Non-ideal actuator dynamics

3.1. *General remarks*

Ideal tracking of the gradient of an artificial potential field was achieved in §2 via sliding mode control, an efficient and practical tool to implement high-gain. In fact, sliding mode control implements infinite gain: while the system is in 'sliding mode', the input to the sliding mode controller (7), the sliding variable s, is identically equal to zero. On the other hand, the average of the output of the controller, $\tilde{f}$, may assume any value in the interval $[-f_0, f_0]$. Consequently, the resulting gain of the sliding mode controller, $K_{\text{smc}} = \tilde{f}/s$, tends to infinity. The average of control, $\tilde{f}$, can be determined using the continuation method by Filippov (1961) or the equivalent control method developed by Utkin (1992). It should be noted that a continuous linear control law $f = -\lambda s$ would lead to similar results in the limit $\lambda \to \infty$ as shown by Utkin (1978). For such a linear control law, actuator saturation should be taken into account, leading to a discontinuous control law similar to (7).

In the presence of unmodelled dynamics, however, the feedback gain should not exceed some finite value, independently of whether a continuous linear controller with a high-gain λ or a discontinuous controller with K_{smc} tending to infinity, are employed. Otherwise, discontinuous control leads to self-oscillations with finite amplitude and bounded frequency, referred to as chattering in the control literature. Moreover, unbounded high-gain control causes instability.

In many practical applications, control discontinuities are dictated by the very nature of the actuator inputs. Typical examples are power converters of electric motors and voltages of the windings controlling the valve position of hydraulic or pneumatic actuators. Usually, a continuous control law is adapted to discontinuous actuator inputs via pulse-width modulation. In the light of recent advances of high-speed switching circuitry and insufficient linear control methodology for internally nonlinear high-order plants, such as AC motors, sliding mode control has become increasingly popular. Implementation of sliding modes by means of most common electronic components is straightforward. Commercially available electronic converters enable handling of switching frequencies in the MHz range. Restricting the functionality of power converters to pulse-width modulation thus seems unjustified. Employing algorithms with discontinuous control actions is promising, since the discontinuities are an inherent part of the converter elements, argued Utkin (1993).

3.2. *Model for actuator dynamics*

For illustration purposes in this paper, we assume a general linear jth order model for the actuators. However, the concepts of eliminating chattering presented below are also applicable to nonlinear actuator dynamics. The dynamics of the actuator generating the force f_x in (1) are taken to be governed by

$$\left.\begin{aligned} \mu \dot{z} &= Az + Bu_x \\ f_x &= Cz \end{aligned}\right\} \tag{14}$$

where $A_{j\times j}$ is assumed to be Hurwitz, $B_{j\times 1}$ and $C_{1\times j}$ are such that $CA^{-1}B = -1$, and μ is a small time constant. We assume that A, B and C are unknown with known order j, and that the pair (A, B) is controllable. The input u_x is truly discontinuous and may

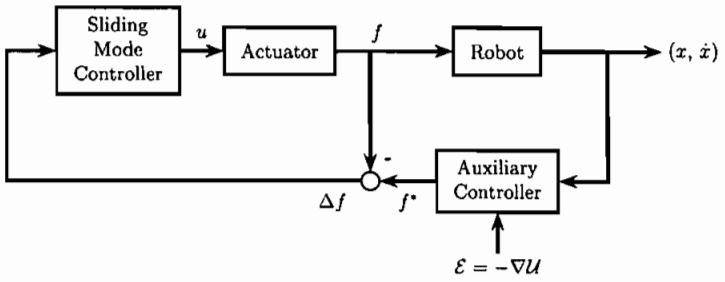

Figure 2. Cascaded control design.

only take two values $u_x \in \{-u_0, +u_0\}$. The output force f_x of (14) is the input to the first row of (1). Similar dynamics are assumed for the actuator generating the force f_y.

3.3. *Cascaded control design*

For systems with measurable actuator outputs $f = [f_x\, f_y]^T$, cascaded control design is appropriate. This method was also referred to as 'control design using regular form' by Luk'yanov and Utkin (1981) and as 'integrator back-stepping', see for example Kokotović (1992). The design procedure consists of two steps: first, an auxillary control law f^* is derived under the assumption that f in the subsystem (1) can be controlled directly. The only constraint for f^* is that its time derivative is bounded according to the (small) time constant μ in (14). In the second step, the actual control u is designed for the actuator subsystem to nullify the error $\Delta f = f^* - f$ despite unknown actuator dynamics, see Fig. 2.

Since the actual control input to the overall system, u, is discontinuous, control design for (14) follows known sliding mode methodology. The sliding manifold comprises the 'actuator output error' Δf and its time derivatives. The details of the design procedure for linear systems like (14) can be found in Chapter 7 of Utkin (1992). Sliding mode control for various types of electrical motors with nonlinear dynamics has been discussed by Utkin (1993).

In many applications, however, the force/torque outputs of the actuators are not measurable. The control algorithm has to compensate for the actuator dynamics implicitly in order to eliminate chattering. In the following, we will illustrate how chattering-free motion can be achieved by using asymptotic observers, in spite of discontinuous control inputs u and without knowledge of the actuator dynamics.

3.4 *Auxiliary observer loop*

This section discusses the utilization of an auxiliary observer loop to eliminate chattering. Despite discontinuous control inputs, chattering triggering by unmodelled dynamics may be suppressed by introducing asymptotic state observers as a bypass for the high-frequency component in the sliding mode control signal. The fundamental idea is to generate ideal sliding mode in the auxiliary observer loop which, since being implemented in the controller, is free of unmodelled dynamics. The behaviour of the actual system is shown to be 'close' to the ideal observer system, with the performance depending on the 'quality' of the observer. In contrast to high-gain control systems with bounds imposed on the gain in the main feedback loop, the bounded-gain conditions are only imposed on the gain of the auxiliary observer. Furthermore, since

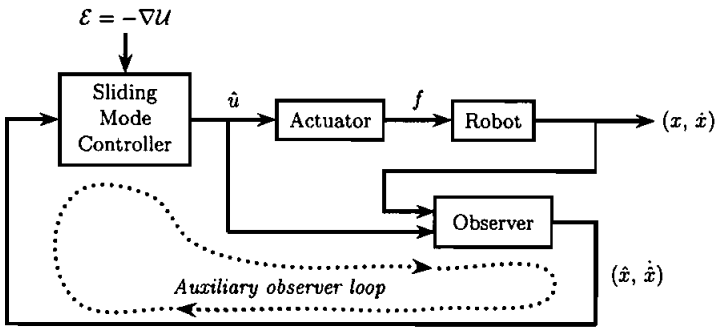

Figure 3. Auxiliary observer loop with ideal sliding mode.

the observer is implemented as a computer routine, no limitations of the feedback control 'resources' apply.

Different observer configurations are possible, depending on the availability of state measurements and knowledge of model parameters. A flow diagram is shown in Fig. 3. The auxiliary observer loop without unmodelled actuator dynamics is depicted with a dotted line. For clarity of presentation, we first illustrate the observer design based on full state feedback and complete knowledge of model parameters. Then, the design is extended to less restrictive conditions. In the following, the development is only detailed for the x-coordinate of (1). It is understood that similar derivations hold for the y-coordinate.

3.4.1. *Full state feedback and complete system knowledge.* For the principle observer design, we assume that the states of the system (1) are available for feedback, and that M and $g(\cdot)$ are known exactly. The observer for $(x, \dot{x})$ is defined as

$$M\ddot{\hat{x}} + g_x(\cdot) = u_x - K_x(l_x\bar{x} + \dot{\bar{x}}) \tag{15}$$

where $\bar{x} = \hat{x} - x$ is the observation error, decaying as determined by the parameters $K_x > 0$ and $l_x > 0$ according to

$$M\ddot{\bar{x}} + K_x(l_x\bar{x} + \dot{\bar{x}}) = (u_x - f_x) \tag{16}$$

The observation error in (16) is perturbed by the term $(u_x - f_x)$. We will later examine the average influence of this perturbation and its effect on the difference between the real system and the auxiliary observer loop.

Control u_x is chosen on the base of the modified sliding manifold

$$\begin{bmatrix} \hat{s}_x \\ \hat{s}_y \end{bmatrix} = \begin{bmatrix} \dot{\hat{x}} \\ \dot{\hat{y}} \end{bmatrix} - v_d(t)\frac{\mathscr{E}(x, y)}{\max(\|\mathscr{E}(x, y)\|, \varepsilon_{\mathscr{E}})} = 0 \tag{17}$$

and, similarly to (7), takes the form

$$u_x = -u_0 \operatorname{sign} \hat{s}_x \tag{18}$$

The appropriate magnitude of control u_0 can be determined by a stability analysis based on a similar procedure as in (8)–(12).

The behaviour of the system, and in particular of the perturbation term $(u_x - f_x)$, can be examined using the equivalent control method, see Chapter 2 of Utkin (1992). Since the observer loop (15) under control (18) is free of unmodelled dynamics, the

ideal sliding mode is initiated after finite time. The states of the observer system (15) are invariantly confined to the modified sliding manifold (17). Solving

$$\dot{s}_x = \frac{u_x}{M} - \left(\dot{v}_d(t) \frac{\mathscr{E}_x}{\max(\|\mathscr{E}\|, \varepsilon_{\mathscr{E}})} + v_d(t) \frac{d}{dt} \left(\frac{\mathscr{E}_x}{\max(\|\mathscr{E}\|, \varepsilon_{\mathscr{E}})} \right) \right) - \frac{K_x}{M} (l_x \bar{x} + \dot{\bar{x}}) = 0 \quad (19)$$

for the control u_x yields the equivalent control

$$\hat{u}_{x_{eq}} = M \left(\dot{v}_d(t) \frac{\mathscr{E}_x}{\max(\|\mathscr{E}\|, \varepsilon_{\mathscr{E}})} + v_d(t) \frac{d}{dt} \left(\frac{\mathscr{E}_x}{\max(\|\mathscr{E}\|, \varepsilon_{\mathscr{E}})} \right) \right) + K_x (l_x \bar{x} + \dot{\bar{x}}) \quad (20)$$

representing a continuous average value of the discontinuous control (18).

The actual system (1) is driven by the input f_x of the actuator dynamics (14) as shown

$$\left. \begin{aligned} \mu \dot{z} &= Az + B\hat{u}_{x_{eq}} \\ f_x &= Cz \end{aligned} \right\} \quad (21)$$

In accordance with singular perturbation theory, it can be shown for small μ and stable dynamics (14) that

$$f_x = \hat{u}_{x_{eq}} + \mathcal{O}(\mu) \quad (22)$$

where $\mathcal{O}(\mu)$ denotes an error of μ-order. Substitution of (22) into (16) reveals that the observer error is of $\mathcal{O}(\mu/K_x)$-order. In other words, the 'real' system (1) with actuator dynamics (14) follows the observer system (15) in ideal sliding mode along (17) with an error of $\mathcal{O}(\mu/K_x)$-order. For (22) to hold, it is vital that the observer dynamics are slower than the actuator dynamics, i.e. $\mu \ll 1/K_x$. Choosing the observer gain too high would excite the unmodelled actuator dynamics, in return, again leading to chattering.

3.4.2. *Full state feedback and parametric uncertainty.* The parameters in (1) have to be estimated by $\hat{m}$ and $\hat{g}(\cdot)$, resulting in errors $\bar{m} = \hat{m} - m$ and $\bar{g} = \hat{g} - g$. Solving $\dot{s}_x = 0$ in (17) for the equivalent control yields

$$\hat{u}_{x_{eq}} = \hat{g}_x + \hat{m} \left(a_d(t) \frac{\mathscr{E}_x}{\max(\|\mathscr{E}\|, \varepsilon_{\mathscr{E}})} + v_d(t) \frac{d}{dt} \left(\frac{\mathscr{E}_x}{\max(\|\mathscr{E}\|, \varepsilon_{\mathscr{E}})} \right) \right) + K_x (l_x \bar{x} + \dot{x}) \quad (23)$$

The observation error becomes

$$\ddot{\bar{x}} + \frac{K_x}{\hat{m}} (l_x \bar{x} + \dot{\bar{x}}) = \left(\frac{g_x}{m} - \frac{\hat{g}_x}{\hat{m}} \right) + \left(\frac{f_x}{m} - \frac{u}{\hat{m}} \right) \quad (24)$$

which, by utilizing (22), can be written as

$$\ddot{\bar{x}} + \frac{K_x}{m} (l_x \bar{x} + \dot{\bar{x}}) = -\frac{\bar{m}}{m} f_x(\cdot) - \frac{\bar{g}_x}{m} + \frac{\mathcal{O}(\mu)}{m} \quad (25)$$

According to (25), the observation error is of $\mathcal{O}(1/K_x)$-order. For choosing the gain K_x, it should be kept in mind that it is necessary to maintain $\mu \ll 1/K_x$ in order to preserve the validity of (22). A trade-off has to be achieved between good tracking performance and eliminating of chattering

3.4.3. *Position feedback and complete system knowledge.* In some situations, velocity feedback might not be available, hence only the absolute position of the robot with respect to the world coordinate system can be used for observer design. For the sake

of lucidity, we again assume complete knowledge of the system parameters. Extension to uncertainty conditions follows similar considerations as above. Denoting $\kappa_1 = x$ and $\kappa_2 = \dot{x}$, the observer is defined as

$$\left.\begin{aligned} \dot{\hat{\kappa}}_1 &= \hat{\kappa}_2 - l_{x_1}(\hat{\kappa}_1 - \kappa_1) \\ \dot{\hat{\kappa}}_2 &= \frac{1}{m}(-g_x(\cdot) + u_x) - l_{x_2} l_{x_1}(\hat{\kappa}_1 - \kappa_1) \end{aligned}\right\} \tag{26}$$

The observation errors $\bar{\kappa}_1 = \hat{\kappa}_1 - \kappa_1$ and $\bar{\kappa}_2 = \hat{\kappa}_2 - \kappa_2$ are governed by

$$\dot{\bar{\kappa}}_1 + l_{x_1}\bar{\kappa}_1 = \bar{\kappa}_2 \tag{27}$$

$$\dot{\bar{\kappa}} + l_{x_2} l_{x_1}\bar{\kappa}_1 = \frac{u_x - f_x}{m} \tag{28}$$

For sufficiently large gain l_{x_1}, $\bar{\kappa}_1$ (27) converges to zero. Exploiting the equivalence of high-gain control and sliding mode control established by Utkin (1978), the equivalent control method can be employed, setting $\dot{\bar{\kappa}}_1$ formally to zero to yield $\bar{\kappa}_2 = l_{x_1}\bar{\kappa}_1$. Substitution of (22) into (28) yields

$$\dot{\bar{\kappa}}_2 + l_{x_2}\bar{\kappa}_2 = -\frac{\mathcal{O}(\mu)}{m} \tag{29}$$

testifying to an observation error of $\mathcal{O}(\mu/l_{x_2})$-order. The rest of the derivations follow from above.

Remark: It should be noted that the control algorithm designed in the previous sections can be also be applied to gradient tracking of n-link manipulators. Moreover, in many industrial robot manipulators, the joint velocities are not measurable, thus an observer of type (26) is mandatory for obtaining estimates of the joint velocities, since differentiation of the joint positions is undesirable. □

4. Non-holonomic kinematics

This section extends the sliding mode control strategy for holonomic mobile robots of type (1) to mobile robots with non-holonomic kinematics. The general idea of control design, to orient the velocity vector of the robot colinear to the planar gradient field $\mathcal{S}(x, y) \in \mathbb{R}^2$, is preserved. However, the control algorithm has to be re-designed to accommodate the non-holonomic motion constraints. A non-holonomic wheel-set is used as a general model of a mobile robot with non-holonomic kinematics.

4.1. *Model of a mobile robot with non-holonomic kinematics*

A typical example of a mobile robot with non-holonomic kinematics is shown in Fig. 4(*a*). The kinematics are determined by a driven and steered front wheel, and two free-turning rear wheels with fixed orientation. The two control inputs are the velocity v and the steering angle θ of the front wheel. A kinematically equivalent configuration is depicted in Fig. 4(*b*) and features two differentially driven rear wheels and a castor front wheel. In this case, the control inputs are the two velocities v_L and v_R of the rear wheels.

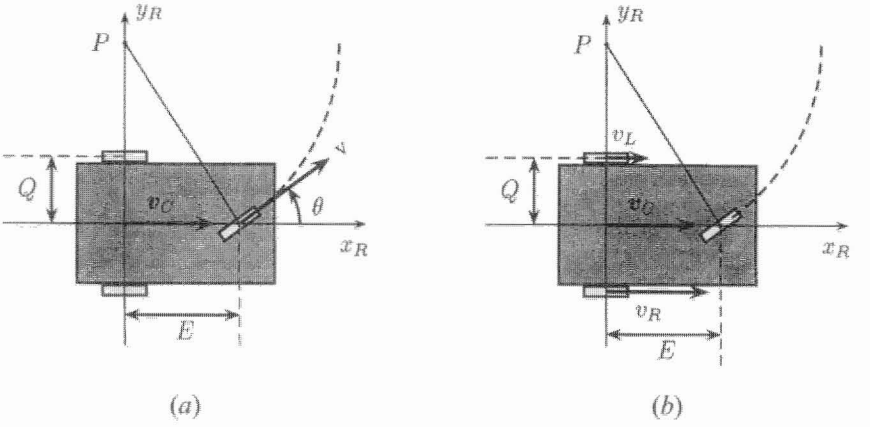

(*a*) (*b*)

Figure 4. Two configurations of tricycle kinematics.

The configurations in Figs 4(*a*) and (*b*) are related via

$$\left.\begin{aligned} v_{\mathrm{L}} &= v\left(\cos\theta - \frac{D}{L}\sin\theta\right) \\ v_{\mathrm{C}} &= v\cos\theta \\ v_{\mathrm{R}} &= v\left(\cos\theta + \frac{D}{L}\sin\theta\right) \end{aligned}\right\} \tag{30}$$

The simplest model for the above non-holonomic kinematics is a single wheel-set consisting the two rear wheels of the mobile robots in Fig. 4 without the stabilizing front wheel. The motion of the centre point of the wheel-set with respect to a fixed workspace frame (x_W, y_W), as depicted in Fig. 5, is given by

$$\left.\begin{aligned} \dot{x} &= \tfrac{1}{2}(v_{\mathrm{R}} + v_{\mathrm{L}})\cos\phi \\ \dot{y} &= \tfrac{1}{2}(v_{\mathrm{R}} + v_{\mathrm{L}})\sin\phi \\ \dot{\phi} &= \frac{1}{2D}(v_{\mathrm{R}} - v_{\mathrm{L}}), \quad \phi \in [-\pi, \pi[\end{aligned}\right\} \tag{31}$$

The planar robot workspace is denoted by $\mathbb{W} \subset \mathbb{R}^2$ and the configuration space $\mathbb{C} \subset \mathbb{R}^3$ is given by $\mathbb{C} = \mathbb{W} \times [-\pi, \pi[$. The configuration space $\mathbb{C}$ comprises the location $(x, y) \in \mathbb{W}$ of the wheel-set and its orientation ϕ. We assume that the robot configuration, also called posture (x, y, ϕ), is available for feedback, and that the distance between the two rear wheels, $2D$, is known.

The wheel-set in Fig. 5 can travel both forward and backward. Forward motion is characterized by $\phi \in [-\pi/2, \pi/2]$ and $v_{\mathrm{C}} > 0$, or equivalently by $\phi \in [-\pi, -\pi/2[\bigcup]\pi/2, \pi[$ and $v_{\mathrm{C}} < 0$, where v_{C} is the velocity of the wheel-set centre. Similarly, backward motion can be achieved via $\phi \in [-\pi/2, \pi/2]$ and $v_{\mathrm{C}} < 0$, or via $\phi \in [-\pi, -\pi/2[\bigcup]\pi/2, \pi[$ and $v_{\mathrm{C}} > 0$. We assume that all angles are given in the range $[-\pi, \pi[$. In particular, the arc-tangent function '$A\tan(\cdot)$' utilized in the following is assumed to return angles within all four quadrants, as opposed to the function '$a\tan(\cdot)$' returning angles in $[-\pi/2, \pi/2[$.

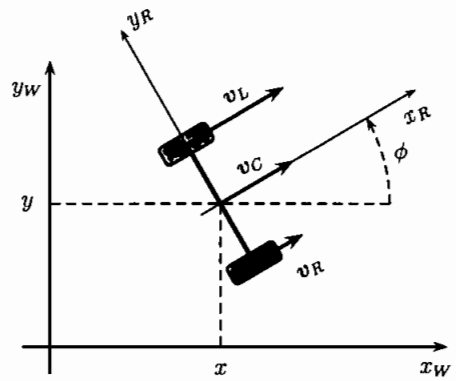

Figure 5. Motion of wheel-set in workspace frame.

The kinematic model (31) can be simplified via (30) to

$$\left.\begin{aligned}\dot{x} &= v_C \cos\phi \\ \dot{y} &= v_C \sin\theta \\ \dot{\phi} &= \omega\end{aligned}\right\} \tag{32}$$

where $\omega = (v/L)\sin\theta$ is the rotation of the wheel-set about the vertical axis. Translation v_C and rotation ω are assumed to be subjected to first-order dynamics of the form

$$M\dot{v}_C + h_v(\cdot) = \Psi \tag{33}$$

$$J\dot{\omega} + h_\omega(\cdot) = \Omega \tag{34}$$

with bounded parameters $M^- < M < M^+$ and $J^- < J < J^+$, and bounded functions $|h_v(\cdot)| \leqslant h_v^+$ and $|h_\omega(\cdot)| \leqslant h_\omega^+$ comprising additional dynamics and additive disturbances. Similar to before, it is assumed that the control inputs can only take two values $\Psi \in \{-\Psi_0, +\Psi_0\}$ and $\Omega \in \{-\Omega_0, +\Omega_0\}$, respectively.

4.2. *Gradient tracking control for a non-holonomic wheel-set*

The goal of control is to orient the velocity vector of the centre of the wheel set, v_C, colinear to the gradient vector $\mathscr{E}(x, y) = -\nabla\mathscr{U}$, with a desired magnitude $v_d(t)$. Due to (32), orientation and velocity of the wheel set can be controlled independently via the inputs Ψ and Ω.

4.2.1. *Velocity control.* The velocity control is based on the sliding manifold

$$s_v = v_d(t) - v_C \tag{35}$$

where the desired velocity $v_d(t)$ was defined in (11) to have bounded acceleration $|a_d(t)| \leqslant a_d^+$, see (12). In order to avoid tedious case studies for forward and backward motion, we assume a positive velocity $v_d(t) > 0$ for all times.

Differentiation of $s_v = 0$ in (35) along the system trajectories (33) yields

$$\dot{s}_v = a_d(t) + \frac{h_v}{M} - \frac{\Psi}{M} \tag{36}$$

The sliding mode along $s_v = 0$ can be enforced using the control

$$\Psi = \Psi_0 \operatorname{sign} s_v \tag{37}$$

for the magnitude of control satisfying $\Psi_0 > (h_v^+ + M^+ a_d^+ + \xi_v)$, for some scalar constant $\xi_0 > 0$. Stability of s_v can be established using a quadratic Lyapunov function $V_v = s_v^2/2$ following the lines of the stability analysis in (8)–(12). It should be noted that the sliding mode occurs immediately for zero initial conditions $s_v(0) = 0$.

As outlined previously, the motion of the wheel set during the sliding mode can be examined using the equivalent control method, see for example, Utkin (1992). Solving $\dot{s}_v = 0$ (36) for the control input Ψ yields

$$\Psi_{eq} = h_v + Ma_d(t) \tag{38}$$

which will be utilized later in the development.

4.2.2. *Orientation control* The orientation error is given by

$$\Delta\phi = A \tan \frac{\mathscr{E}_y(x,y)}{\mathscr{E}_x(x,y)} - \phi = \phi_d(x,y) - \phi \tag{39}$$

The sliding mode controller used to drive (39) to zero is based on the sliding manifold

$$s_\phi = c_\phi \Delta\phi + \frac{d}{dt}(\Delta\phi) \tag{40}$$

for some scalar parameter $c_\phi > 0$. Differentiation along the system trajectories (32) and (34) yields

$$\dot{s}_\phi = c_\phi \dot{\phi}_d - c_\phi \omega + \ddot{\phi}_d + \frac{1}{J}(h_\omega - \Omega) \tag{41}$$

The time-derivatives of $\phi_d = A \tan(\mathscr{E}_x(x,y)/\mathscr{E}_y(x,y))$ in the course of motion are

$$\dot{\phi}_d = \frac{d}{dt}\left(A \tan \frac{\mathscr{E}_y(x,y)}{\mathscr{E}_x(x,y)}\right) = F_0 v_C \tag{42}$$

$$\begin{aligned} \ddot{\phi}_d &= \frac{d^2}{dt^2}\left(A \tan \frac{\mathscr{E}_y(x,y)}{\mathscr{E}_x(x,y)}\right) \\ &= F_1 + \frac{F_0}{M}\Psi \\ &= F_2 + F_0 a_d \end{aligned} \tag{43}$$

where

$$F_0 = \frac{\varepsilon_x^2 [D_x + D_y](\mathscr{E}_y) - \mathscr{E}_x \mathscr{E}_y [D_x + D_y](\mathscr{E}_x)}{\|\mathscr{E}\|^2}$$

$$F_1 = v_C^2 F_2 - \frac{h_v}{M} F_0$$

$$\begin{aligned} F_2 = \mathscr{E}_x \Bigg\{ & \frac{1}{\|\mathscr{E}\|^4}[2\mathscr{E}_x [D_x](\mathscr{E}_x)[D_x + D_y]\mathscr{E}_y + \mathscr{E}_x^2 [D_{xx} + D_{xy}](\mathscr{E}_y) \\ & - \mathscr{E}_y [D_x^2 + D_x D_y](\mathscr{E}_x) - \mathscr{E}_x [D_x](\mathscr{E}_y)[D_x + D_y](\mathscr{E}_x) - \mathscr{E}_x \mathscr{E}_y [D_{xx} + D_{xy}](\mathscr{E}_x)] \\ & - \frac{3}{\|\mathscr{E}\|^6}[\mathscr{E}_x^2 [D_x + D_y](\mathscr{E}_y) - \mathscr{E}_x \mathscr{E}_y [D_x + D_y](\mathscr{E}_x)][\mathscr{E}_x [D_x](\mathscr{E}_x) + \mathscr{E}_y [D_x](\mathscr{E}_y)] \Bigg\} \\ & + \mathscr{E}_y \Bigg\{ \frac{1}{\|\mathscr{E}\|^4}[2\mathscr{E}_x [D_y](\mathscr{E}_x)[D_x + D_y](\mathscr{E}_y) + \mathscr{E}_x^2 [D_{xy} + D_{yy}](\mathscr{E}_y) \end{aligned}$$

$$-\mathscr{E}_y[D_x D_y + D_y^2](\mathscr{E}_x) - \mathscr{E}_x[D_y](\mathscr{E}_y)[D_x + D_y](\mathscr{E}_x) - \mathscr{E}_x\mathscr{E}_y[D_{xy} + D_{yy}](\mathscr{E}_x)]$$
$$-\frac{3}{\|\mathscr{E}\|^6}[\mathscr{E}_x^2[D_x + D_y](\mathscr{E}_y) - \mathscr{E}_x\mathscr{E}_y[D_x + D_y](\mathscr{E}_x)][\mathscr{E}_x[D_y](\mathscr{E}_x) + \mathscr{E}_y[D_y](\mathscr{E}_y)]\Big\}$$

are upper bounded by F_0^+, F_1^+ and F_2^+, respectively. $[D_x](\cdot)$ denotes the differentiation operator $\partial(\cdot)/\partial x$, $[D_{xx}](\cdot)$ denotes the differentiation operator $\partial^2(\cdot)/\partial x^2$, and $[D_{xy}](\cdot)$ denotes the differentiation operator $\partial^2(\cdot)/\partial x \partial y$. Similar terminology was used for differentiation with respect to y. Equivalent control (38) for the velocity control Ψ has been substituted to reduce expression (43).

Similarly to the control design in (37), the orientation control Ω for (41) is defined as

$$\Omega = \Omega_0 \operatorname{sign} s_\phi \tag{44}$$

with

$$\Omega_0 > \left(h_\omega^+ + J^+\left(F_1^+ + \frac{F_2^+}{M^-}\Psi_0 + c_\phi(F_0^+ v_C + \omega^+)\right) + \xi_\phi\right)$$

for some scalar constant $\xi_\phi > 0$. Convergence of s_ϕ to zero within finite time, manifested via the Lyapunov function $V_\phi = s_\phi^2/2$, implies subsequent convergence of $\Delta\phi$ to zero at the rate specified by c_ϕ in (40). Once again, the transient phase is omitted for zero initial conditions.

4.2.3. *Implementation.* The quantities Ψ and Ω are not the real control inputs for the mobile robots shown in Fig. 4. Instead, either velocity v and steering angle θ of the front wheel, or alternatively the velocities v_L and v_R of the rear wheels are the real control inputs. In contrast to continuous control, the transformation of the discontinuous control is not straightforward. Let us consider the input vector $[v_L \; v_R]^T$ as an example for such a transformation.

We assume inertial dynamics for the wheel velocities of the general form

$$\begin{aligned} M_R \dot{v}_R &= h_R(\cdot) + w_R \\ M_L \dot{v}_L &= h_L(\cdot) + w_L \end{aligned} \tag{45}$$

with bounded M_R, M_L, $h_R(\cdot)$ and $h_L(\cdot)$. Substitution of (45) into the time derivatives of the sliding manifolds $s_v = 0$ in (35) and $s_\phi = 0$ in (40) yields

$$\left.\begin{aligned} \dot{s}_v &= a_d - \frac{1}{2}\left(\frac{h_R(\cdot)}{M_R} + \frac{h_L(\cdot)}{M_L}\right) - w_v \\ \dot{s}_\phi &= c_\phi \frac{d}{dt}(\Delta\phi) + \ddot{\phi}_d - \frac{c_\phi}{2D}\left(\frac{h_R(\cdot)}{M_R} + \frac{h_L(\cdot)}{M_L}\right) - w_\phi \end{aligned}\right\} \tag{46}$$

where the auxiliary controls w_v and w_ϕ are defined as

$$\begin{bmatrix} w_v \\ w_\phi \end{bmatrix} = \frac{1}{2}K\begin{bmatrix} w_R \\ w_L \end{bmatrix}, \quad K = \begin{bmatrix} \dfrac{1}{M_R} & \dfrac{1}{M_L} \\ \dfrac{1}{DM_R} & -\dfrac{1}{DM_L} \end{bmatrix} \tag{47}$$

Similar to before, the control laws are defined as

$$\left.\begin{aligned} w_{\mathrm{v}} &= w_{\mathrm{v}_0} \operatorname{sign} s_{\mathrm{v}} \\ w_{\phi} &= w_{\phi_0} \operatorname{sign} s_{\phi} \end{aligned}\right\} \tag{48}$$

for

$$w_{\mathrm{v}_0} > \left[a_{\mathrm{d}}^{+} + \frac{1}{2}\left(\frac{h_{\mathrm{R}}^{+}(\cdot)}{M_{\mathrm{R}}^{-}} + \frac{h_{\mathrm{L}}^{+}(\cdot)}{M_{\mathrm{L}}^{-}} \right) + \xi_{\mathrm{v}} \right]$$

$$w_{\phi_0} > \left[c_{\phi}(F_0^{+} v_{\mathrm{C}} + \omega^{+}) + \frac{1}{2D}\left(\frac{h_{\mathrm{R}}^{+}(\cdot)}{M_{\mathrm{R}}^{-}} + \frac{h_{\mathrm{L}}^{+}(\cdot)}{M_{\mathrm{L}}^{-}} \right) + \xi_{\phi} \right]$$

and some positive scalars ξ_{v} and ξ_{ϕ}. The stability analysis follows from previous considerations.

Under the assumption that each of the control inputs for w_{R} and w_{L} can only take two values, $w_{\mathrm{R}} = \{-w_{\mathrm{R}_0}, +w_{\mathrm{R}_0}\}$ and $w_{\mathrm{L}} = \{-w_{\mathrm{L}_0}, +w_{\mathrm{L}_0}\}$, control (48) cannot be realized directly with (47). Special measures have to be taken to derive appropriate control laws for w_{R} and w_{L}. A suitable technique exploits the properties of the equivalent control method for non-singular K. We define an auxiliary state $\eta \in \mathbb{R}^2$ as

$$\begin{bmatrix} \dot{\eta}_1 \\ \dot{\eta}_2 \end{bmatrix} = 2K^{-1} \begin{bmatrix} w_{\mathrm{v}} \\ w_{\phi} \end{bmatrix} - \begin{bmatrix} w_{\mathrm{R}} \\ w_{\mathrm{L}} \end{bmatrix} \tag{49}$$

with the control being

$$w_{\mathrm{R}} = w_{\mathrm{R}_0} \operatorname{sign} \eta_1, \quad w_{\mathrm{L}} = w_{\mathrm{L}_0} \operatorname{sign} \eta_2 \tag{50}$$

There exist finite values of w_{R_0} and w_{L_0} such that the sliding mode is enforced along $\eta = 0$ despite discontinuous 'disturbances' w_{v} and w_{ϕ}. Direct application of the equivalent control method shows that the transformation (47) is realized exactly.

In the case of non-ideal actuator dynamics for $[w_{\mathrm{R}}\ w_{\mathrm{L}}]^{\mathrm{T}}$, the observer-based chattering elimination method presented in §3 can be employed. The details of this procedure are omitted here since they involve little that is new to the above.

5. Conclusions

Artificial potential fields are an elegant tool for navigation control and obstacle avoidance of robotic systems. In order to guarantee safe operation, good tracking of the gradient lines of the artificial potential field is indispensable. This paper presented a sliding mode controller yielding exact gradient tracking by orienting the velocity vector colinear to the gradient. Special emphasis was placed on elimination of chattering triggered by unmodelled actuator dynamics. An auxiliary observer loop served as a bypass for the high-frequency component in the sliding mode control signal. The ideal sliding mode was generated in the auxiliary observer loop, the behaviour of the actual system being 'close' to the observer system. A second important topic was non-holonomic motion constraints, requiring reconsideration of the control strategy. Decoupling of translational and rotational motion via intermediate control variables served as the basis for control design for mobile robots with tricycle kinematics.

Acknowledgments

The authors are indebted to Professor Jürgen Ackermann of DLR, Germany, and to Professor Fumio Harashima and Professor Hideki Hashimoto, both with Tokyo University, Japan, for their encouragement and support. Jürgen Guldner thanks DAAD, the German Academic Exchange Council, for their financial support for visiting Tokyo University in summer 1994. Vadim I. Utkin is grateful to the Toshiba Co. for supporting this research during his stay at Tokyo University in 1994. Most importantly, the insightful comments of the anonymous reviewers are highly appreciated.

References

DeCarlo, R. A., Zak, S. H., and Matthews, G. P., 1988, Variable structure control of nonlinear multivariable systems: a tutorial. *Proceedings of the Institute of Electrical and Electronics Engineers*, **76**, 212–232.

Filippov, A. F., 1961, Application of the theory of differential equations with discontinuous right-hand sides to non-linear problems of automatic control. *Proceedings of the 1st IFAC Congress*, Vol. II (London, U.K.: Butterworths), pp. 923–927.

Guldner, J., and Utkin, V. I., 1993, Sliding mode control for an obstacle avoidance strategy based on an electrical potential field. *Proceedings of the IEEE Conference Decision and Control*, San Antonio, Texas, U.S.A., pp. 424–429; 1995, Sliding mode control for gradient tracking and robot navigation using artificial potential fields. *IEEE Transactions on Robotics and Automation*, **11**(2), 247–254.

Hashimoto, H., Harashima, F., Utkin, V. I., Krasnova, S. A., and Kaliko, I. M., 1993, Sliding mode control and potential fields in obstacle avoidance. *Proceedings of the European Control Conference*, Groningen, The Netherlands, pp. 859–862.

Hogan, N., 1985, Impedance control: an approach to manipulation—Parts I–III. *ASME Journal of Dynamic Systems, Measurement and Control*, **107**, 1–24.

Khatib, O., 1986, Real-time obstacle avoidance for manipulators and mobile robots. *International Journal of Robotics Research*, **5**, 90–98.

Khosla, P., and Volpe, R., 1988, Superquadratic artificial potentials for obstacle avoidance and approach. In *Proceedings of the IEEE Conference on Robotics and Automation*. Philadelphia, Pennsylvania, U.S.A., pp. 1778–1784.

Koditschek, D. E., 1987, Exact robot navigation by means of potential functions: some topological considerations. *Proceedings of the IEEE Conference on Robotics and Automation*. Raleigh, North Carolina, U.S.A., pp. 1–6; 1991a, The control of natural motion in mechanical systems. *ASME Journal of Dynamic Systems, Measurement and Control*, **113**, 547–551; 1991b, Some applications of natural motion control. *ASME Journal of Dynamic Systems, Measurement and Control*, **113**, 552–557.

Kokotović, P. V., 1992, The joy of feedback: nonlinear and adaptive. *IEEE Control Systems*, June, pp. 7–17.

Luk'yanov, A. G., and Utkin, V. I., 1981, methods of reducing equations for dynamic systems to a regular form. *Automation and Remote Control*, **42**, 413–420.

Rimon, E., and Koditschek, D. E., 1992, Exact robot navigation using artificial potential functions. *IEEE Transactions on Robotics and Automation*, **8**, 501–518.

Utkin, V. I., 1978, Application of equivalent control method to systems with large feedback gain. *IEEE Transactions on Automatic Control*, **23**, 484–486; 1992, *Sliding Modes in Control and Optimization* (Berlin, Germany: Springer-Verlag); 1993, Sliding mode control design principles and applications to electric drives. *IEEE Transactions on Industrial Electronics*, **40**, 23–36.

Utkin, V. I., Drakunov, S., Hashimoto, H., and Harashima, F., 1991, Robot path obstacle avoidance control via sliding mode approach. *Proceedings of the IEEE/RSJ International Workshop on Intelligent Robots and Systems*. Osaka, Japan, pp. 1287–1290.

Volpe, R., and Khosla, P., 1987, Artificial potentials with elliptical isopotential contours for obstacle avoidance. In *Proceedings of the IEEE Conference Decision and Control*. Los Angeles, California, U.S.A., pp. 180–185.